All autoimmune pancreatitis lesions showed mild, moderate, or marked enhancement throughout almost the entire lesion in both the early and delayed phases of contrast-enhanced harmonic gray scale sonography. Marked enhancement was observed in 2 of the 6 autoimmune pancreatitis lesions, moderate enhancement in 3 of the 6 lesions, and mild enhancement in the remaining lesion. The grade of vascularity of each lesion was the same in both the early and delayed phases of contrast-enhanced harmonic gray scale sonography (Table 1). All autoimmune pancreatitis lesions appeared hypervascular or isovascular throughout the entire lesions in both the early and delayed phase CT images. One of the 6 autoimmune pancreatitis lesions appeared hypervascular in the early phase and isovascular in the delayed phase, and the other 5 appeared isovascular in both phases of the CT images. A hypovascular capsulelike rim at the periphery of the lesion was observed in only 1 of the 6 lesions on the CT images, and it showed marked enhancement on contrast-enhanced harmonic gray scale sonography.

Comparison Between Contrast-Enhanced Harmonic Gray Scale Sonographic Findings and Pathologic Findings

Two of the 6 lesions showed mild fibrosis and severe inflammation, and they exhibited marked enhancement. Three of the 6 lesions showed moderate fibrosis and moderate inflammation, and they exhibited moderate enhancement. The remaining lesion showed severe fibrosis and mild inflammation, and it exhibited mild enhancement (Table 2).

Comparison Between Helical CT Findings and Pathologic Findings

Only 1 of the 6 lesions, a lesion characterized by mild fibrosis and severe inflammation, appeared to be hypervascular in the arterial phase of helical CT. The remaining 5 lesions (1 lesion with mild fibrosis and severe inflammation, 3 lesions with moderate fibrosis with moderate inflammation, and 1 lesion with severe fibrosis and mild inflammation) appeared to be isovascular in the arterial phase of helical CT (Table 2).

Contrast-Enhanced Harmonic Gray Scale Sonographic Findings During and After Steroid Therapy

Three of the 6 patients were treated with corticosteroids (Table 3). Four weeks after the start of steroid therapy, all lesions had decreased in size, and the diameter of the dilated common bile duct had decreased on the basis of conventional sonographic findings. The grade of vascularity on contrast-enhanced harmonic gray scale sonographic images had decreased from marked enhancement to moderate enhancement in 1 case and from moderate enhancement to mild enhancement in 2 cases (Figure 3). At the end of steroid therapy, all mass lesions had further decreased in size, and the common bile duct diameter had also further decreased on the basis of the conventional sonographic findings. The final grade of vascularity on the contrast-enhanced harmonic gray scale sonographic images was mild enhancement in all 3 lesions. No recurrence of pancreatitis was observed during the 1 to 2 years of follow-up in these 3 patients.

Discussion

Pancreatic carcinoma is the most common type of pancreatic tumor, whereas autoimmune pancreatitis is a rare type of pancreatitis characterized by enlargement of all or part of the pancreas and irregular stenosis of the pancreatic ductal system ("sclerosing" pancreatitis) secondary to autoimmune processes.[1] However, autoimmune pancreatitis is frequently detected as a result of

Table 1. Results of Contrast-Enhanced Harmonic Gray Scale Sonography of Autoimmune Pancreatitis (n = 6) in Comparison With Helical CT

	Contrast-Enhanced Harmonic Gray Scale Sonographic Findings, n (%)				Helical CT Findings, n (%)		
Phase	Marked Enhancement	Moderate Enhancement	Mild Enhancement	No Enhancement	Hypervascular	Isovascular	Hypovascular
Early	2 (33)	3 (50)	1 (17)	0 (0)	1 (17)*	5 (83)	0 (0)
Delayed	2 (33)	3 (50)	1 (17)	0 (0)	0 (0)	6 (100)	0 (0)

*This lesion showed hypervascular enhancement with a hypovascular capsulelike rim on the early phase helical CT image.

Table 2. Results of Contrast-Enhanced Harmonic Gray Scale Sonography of Autoimmune Pancreatitis (n = 6) in Comparison With the Pathologic Findings

Case	Contrast-Enhanced Harmonic Gray Scale Sonographic Findings (Early Phase)	Helical CT Findings (Early Phase)	Pathologic Findings	
			Fibrosis	Inflammation
1*	Marked enhancement	Hypervascular	Mild	Severe
2†	Marked enhancement	Isovascular	Mild	Severe
3*	Moderate enhancement	Isovascular	Moderate	Moderate
4†	Moderate enhancement	Isovascular	Moderate	Moderate
5†	Moderate enhancement	Isovascular	Moderate	Moderate
6‡	Mild enhancement	Isovascular	Severe	Mild

*Pathologic findings from surgery.
†Pathologic findings from aspiration biopsy.
‡Pathologic findings from open biopsy.

jaundice caused by narrowing of the common bile duct due to inflammation. Because steroid therapy is effective against autoimmune pancreatitis,[1,2] accurate diagnosis avoids unnecessary resection.

It has been shown that pancreatic carcinoma lesions are not enhanced throughout the entire tumor in the early phase of contrast-enhanced harmonic gray scale sonography,[9] but they often show peripancreatic vessel involvement and dilatation of the main pancreatic duct.[10] In our study, some degree of hypervascular enhancement was observed throughout almost the entire lesion on contrast-enhanced harmonic gray scale sonographic images in all our cases, and they all showed dilatation of the common bile duct without dilatation of the main pancreatic or peripancreatic vessel involvement. We think that these findings may be useful for the diagnosis of autoimmune pancreatitis lesions.

Kim et al[11] reported lymphocyte infiltration, fibrosis, and reduction of glandular elements in 7 patients with pancreatic masses secondary to chronic pancreatitis. It has been shown that inflammatory changes require blood flow, which produces hypervascularity.[12] Koito et al[12] reported that the inflammatory pancreatic masses of 19 of 20 patients were isovascular on carbon dioxide–enhanced sonographic images, and the remaining mass was hypovascular; that hypovascular mass was in a patient with severe fibrosis pathologically. Severe fibrosis can replace pancreatic acinar cells and can inhibit vascular development in an inflammatory lesion, which is probably the reason why 1 inflammatory pancreatic mass in their case series was hypovascular.[12] The vascularity on contrast-enhanced harmonic gray scale sonography in our small series of 6 patients appeared to be positively correlated with the degree of inflammation and inversely correlated with the degree of fibrosis. We also found that contrast-enhanced harmonic gray scale sonography could be useful as a means of monitoring the therapeutic effectiveness of steroid therapy for deciding whether to discontinue treatment. In 3 cases that were treated with corticosteroids in our study, the vascularity on the contrast-enhanced harmonic gray scale sonographic images decreased, and the decrease may have been due to the decrease in inflammation in response to the steroid.[13,14] These findings also support our hypothesis that the degree of inflammation correlated with that of the vascularity on contrast-enhanced harmonic gray scale sonographic images.

There was a discrepancy between the vascularity of the lesions on the contrast-enhanced harmonic gray scale sonographic images and that on the CT images. One difference between these imaging techniques may be that the sonographic contrast agent remains within the blood vessels, whereas the CT contrast agent is distributed

Table 3. Results of Size of the Mass Lesion and Diameter of the Common Bile Duct in Patients With Autoimmune Pancreatitis (n = 3) During and After Steroid Therapy

Case	Size of Mass Lesion, mm			Diameter of Common Bile Duct, mm		
	Before*	4 wk†	End‡	Before*	4 wk†	End‡
1	30	25	22	9	6	4
2	38	35	28	11	9	6
3*	42	33	30	14	10	7
Mean ± SD	37 ± 6	31 ± 5	27 ± 4	11 ± 3	8 ± 2	6 ± 2

*Before steroid therapy.
†Four weeks after the start of steroid therapy.
‡At the end of steroid therapy.

throughout the tissues.[10] The kinetics of contrast agent passage differed between CT and sonographic contrast agents. Second, we examined contrast-enhanced harmonic gray scale sonographic images for the presence or absence of enhancement in the early and delayed phases, whereas on the helical CT images we compared the vascularity of pancreatic mass lesions with that of the surrounding pancreas in the early and delayed phases.[9]

There were several limitations in this study. First, abdominal gas sometimes prevents visualization of pancreatic lesions by contrast-enhanced harmonic gray scale sonography, and it is of limited value for evaluation of lesions in the body and tail of the pancreas. Second, the single plane of the sonographic image sometimes does not visualize the entire normal parenchyma of the pancreas, which makes it difficult to compare the vascularity of pancreatic masses with that of normal parenchyma by contrast-enhanced harmonic gray scale sonography. Therefore, in this study we compared the lesion before enhancement with hypervascular enhancement during the early and delayed phases of contrast-enhanced harmonic gray scale sonography. Third, our grading of vascularity using contrast-enhanced harmonic gray scale sonography is by a subjective method, and the development of a quantitative grading scheme may be required to eliminate this limitation. Fourth, because our study population was small, a study in a larger population of autoimmune pancreatitis lesions is needed to definitely establish the correlation between the pathologic findings and the vascularity observed during contrast-enhanced harmonic gray scale sonography of these lesions.

In conclusion, contrast-enhanced harmonic gray scale sonography may be a sensitive tool for evaluating the vascularity of autoimmune pancreatitis lesions and may be a good indicator for evaluating the therapeutic efficacy of steroid therapy.

References

1. Koga Y, Yamaguchi K, Sugitani A, Chijiiwa K, Tanaka M. Autoimmune pancreatitis starting as a localized form. J Gastroenterol 2002; 37:133–137.
2. Yoshida K, Toki F, Takeuchi T, Watanabe S, Shiratori K, Hayashi N. Chronic pancreatitis caused by an autoimmune abnormality: proposal of the concept of autoimmune pancreatitis. Dig Dis Sci 1995; 40: 1561–1568.
3. Irie H, Honda H, Baba S, et al. Autoimmune pancreatitis: CT and MR characteristics. AJR Am J Roentgenol 1998; 170:1323–1327.
4. Furukawa N, Muranaka T, Yasumori K, Matsubayashi R, Hayashida K, Arita Y. Autoimmune pancreatitis: radiologic findings in 3 histologically proven cases. J Comput Assist Tomogr 1998; 22:880–883.
5. Servais A, Pestieau SR, Detry O, et al. Autoimmune pancreatitis mimicking cancer of the head of pancreas: reports of 2 cases. Acta Gastroenterol Belg 2001; 64:227–230.
6. Taniguchi T, Seko S, Azuma K, et al. Autoimmune pancreatitis detected as a mass in the head of the pancreas with contiguous fibrosis around the superior mesenteric artery. Dig Dis Sci 2001; 46:187–191.
7. Horiuchi A, Kawa S, Hamano H, Hayama M, Ota H, Kiyosawa K. ERCP features in 27 patients with autoimmune pancreatitis. Gastrointest Endosc 2002; 55:494–499.
8. Oshikawa O, Tanaka S, Ioka T, Nakaizumi A, Hamada Y, Mitani T. Dynamic sonography of pancreatic tumors: comparison with dynamic CT. AJR Am J Roentgenol 2002; 178:1133–1137.
9. Ozawa Y, Numata K, Tanaka K, et al. Contrast-enhanced sonography of small pancreatic mass lesions. J Ultrasound Med 2002; 21:983–991.
10. Baert AL, Rigauts H, Marchal G. Ductal adenocarcinoma. In: Baert AL (ed). Radiology of the Pancreas. Berlin, Germany: Springer-Verlag, 1994:129–172.
11. Kim T, Murakami T, Takamura M, et al. Pancreatic mass due to chronic pancreatitis: correlation of CT and MR imaging features with pathologic findings. AJR Am J Roentgenol 2001; 177:367–371.
12. Koito K, Namieno T, Nagakawa T, Morita K. Inflammatory pancreatic masses: differentiation from ductal carcinomas with contrast-enhanced sonography using carbon dioxide microbubbles. AJR Am J Roentgenol 1997; 169:1263–1267.
13. Saito T, Tanaka S, Yoshida H, et al. A case of autoimmune pancreatitis responding to steroid therapy: evidence of histologic recovery. Pancreatology 2002; 2:550–556.
14. Hoshino M, Takahashi M, Takai Y, Sim J, Aoike N. Inhaled corticosteroids decrease vascularity of the bronchial mucosa in patients with asthma. Clin Exp Allergy 2001; 31:722–730.

Noninvasive Assessment of Tumor Vascularity by Contrast-Enhanced Ultrasonography and the Prognosis of Patients with Nonresectable Pancreatic Carcinoma

Takahiro Masaki, M.D.
Shinichi Ohkawa, M.D.
Ayumi Amano, M.D.
Makoto Ueno, M.D.
Kaoru Miyakawa, M.D.
Kazuo Tarao, M.D.

Department of Gastroenterology, Kanagawa Cancer Center Hospital, Yokohama, Japan.

Supported by the Fund for Cancer Research from Kanagawa Prefecture.

The authors thank Dr. Naoyuki Okamoto, Department of Epidemiology, Kanagawa Cancer Center Research Institute, for his statistical consultation.

Address for reprints: Takahiro Masaki, M.D., Department of Gastroenterology, Kanagawa Cancer Center Hospital 1-1-2, Nakao, Asahi-ku, Yokohama, 241-0815, Japan; Fax: (011) 81 453614692; E-mail: tmasaki@nih.go.jp

Received June 15, 2004; revision received September 17, 2004; accepted September 26, 2004.

BACKGROUND. Studies have shown that angiogenesis is one of the factors that influences the prognosis of patients with solid tumors, including pancreatic carcinomas. However, none have assessed noninvasively the relation between angiogenesis and prognosis in patients with pancreatic carcinoma. Contrast-enhanced ultrasonography (US) not only is a convenient, harmless, and noninvasive imaging modality, but it also provides detailed information on tumor vascularity. The objectives of this study were to assess the vascularity of pancreatic carcinoma noninvasively by contrast-enhanced US and to clarify the prognostic value of tumor vascularity in patients with nonresectable pancreatic carcinoma.

METHODS. Thirty-five consecutive patients with pathologically confirmed, nonresectable pancreatic carcinoma were examined with contrast-enhanced US before systemic chemotherapy. The correlations among tumor vascularity, clinicopathologic factors, and clinical outcomes then were analyzed statistically to investigate prognostic indicators.

RESULTS. The median time to progression (TTP) was longer in patients who had avascular tumors compared with patients who had vascular tumors (110 days vs. 28 days, respectively; $P = 0.0072$; log-rank test). The median survival also was longer in patients who had avascular tumors (267 days vs. 115 days, respectively; $P = 0.0034$; log-rank test). A multivariate analysis using a Cox proportional hazards model revealed that tumor vascularity was a significant, independent factor that influenced TTP ($P < 0.001$) and survival ($P = 0.022$) along with primary tumor size and serum lactate dehydrogenase (LDH) level, which are well known as prognostic factors in patients with pancreatic carcinoma.

CONCLUSIONS. The current results indicated that contrast-enhanced US may be useful in assessing the prognosis of patients with nonresectable pancreatic carcinoma who receive systemic chemotherapy. *Cancer* 2005;103:1026–35.
© 2005 American Cancer Society.

KEYWORDS: pancreatic carcinoma, contrast-enhanced ultrasonography, tumor vascularity, noninvasive assessment, prognostic factor, survival, time to progression, chemotherapy.

The incidence of pancreatic carcinoma has increased steadily over the last 4 decades, and this tumor now ranks as the fifth leading cause of cancer death in Japan. Despite an increased understanding of the biology of pancreatic carcinoma, the 5-year survival rate is < 5%, the worst in the Surveillance, Epidemiology, and End Results data base. This poor survival rate is attributed to the high incidence of metastatic disease at diagnosis and the relative chemoresistance of

DOI 10.1002/cncr.20875
Published online 25 January 2005 in Wiley InterScience (www.interscience.wiley.com)

this tumor. Therefore, improvement in the outcome of patients with pancreatic carcinoma depends on the development of effective systemic therapies. Gemcitabine is the most common cytotoxic agent used for this disease. However, the objective response rate of patients with pancreatic carcinoma who are treated with this drug is < 10%.[1,2] Thus, numerous clinical trials of systemic chemotherapy that include combinations of gemcitabine and other antitumor agents have been introduced in an attempt to improve the response rate and survival of patients with advanced pancreatic carcinoma.[3-7] However, we have found that even identical chemotherapy regimens bring about different outcomes in different patients. That is, some patients show improvements in survival and tumor response, whereas others only suffer from inconvenience and increased toxicity. It has been suggested that the burden of treatment should not be added to the suffering of those with advanced pancreatic carcinoma. Therefore, the identification of prognostic factors before treatment would be helpful in selecting the subgroups of patients for which chemotherapy improves survival and in determining efficient treatment strategies with reference to expected survival.

Recently, several studies have shown that angiogenesis is an important factor in the growth, progression, and metastasis of solid tumors, including pancreatic carcinomas,[8-11] and increases in tumor vessel count and in the expression of angiogenic factors, such as vascular endothelial growth factor (VEGF), have been associated with a poor prognosis in patients with pancreatic carcinoma.[12-14] However, all of those studies were conducted on patients who had undergone surgery, and no reports assessing noninvasively the association of angiogenesis with the prognosis of patients with pancreatic carcinoma have been published.

Contrast-enhanced ultrasonography (US) with the contrast agent Levovist (Schering AG, Berlin, Germany) can offer detailed information on tumor vascularity[15-17] and recently has been used to assess the vascularity of pancreatic tumors for differential diagnosis.[18-22] Therefore, the objectives of the current study were to assess the vascularity of pancreatic carcinoma noninvasively with contrast-enhanced US and to clarify the prognostic value of tumor vascularity in patients with nonresectable pancreatic carcinoma.

MATERIALS AND METHODS

Patients

The study included 35 consecutive patients with metastatic or locally advanced, inoperable pancreatic carcinoma and a baseline Karnofsky performance status $\geq$ 60%. These patients were treated by systemic chemotherapy at the Kanagawa Cancer Center Hospital, Kanagawa, Japan, between August, 2001 and February, 2004. US images, computed tomography (CT) scans, and chest X-rays were obtained as pretreatment staging studies to assess the local extension of the tumor and the presence of distant metastasis. Patients who had received previous chemotherapy or radiotherapy were excluded from the analysis. Pathologic confirmation of adenocarcinoma was obtained in all patients by surgical procedures or by fine-needle aspiration biopsy (Sonopsy; Hakko, Tokyo, Japan). All patients with obstructive jaundice underwent percutaneous transhepatic or endoscopic retrograde biliary drainage before chemotherapy.

Contrast Agent

All patients were injected with the US contrast agent, Levovist, which is composed of 99.9% galactose and 0.1% palmitic acid. The agent (2.5 g) was shaken for about 10 seconds with 7 mL of sterile water to yield an opalescent suspension of air microbubbles. The suspension was equilibrated for a few minutes and then was injected manually through a 20-gauge cannula placed into the antecubital vein as a bolus infusion (300 mg/mL of contrast agent; approximately 7 mL in total). After the bolus injection of Levovist, a 0.9% saline solution was infused continuously at 5.0 mL per minute.

US Examination

We used a sonographic scanner (Sequoia 512; Acuson Corporation, Mountain View, CA) with a 4C1 curvilinear array transducer in the harmonic imaging mode, which transmits 2 MHz and receives 4 MHz of sound. We observed the pancreatic tumors from 5 seconds before to 60 seconds after the administration of Levovist, with a frame rate of 1–2 Hz at a mechanical index of 1.5. While imaging tumors, we fixed the transducer at the position where the tumor was drawn initially. US images were recorded continuously on videotape.

US Image Analysis

The US images were analyzed macroscopically for the presence and distribution of tumor vascularity. Patterns of tumor vascularity were described as diffuse enhancement if a vascular signal was identified throughout the lesion, as spotty enhancement if a microbubble signal was observed in part of the tumor, and as no enhancement if parenchymal flow was absent or was detectable only minimally (Fig. 1). In the next step, all images recorded on videotape were changed into digital data by Power Director software (version 2.0; CyberLink Corporation, Tokyo, Japan) in

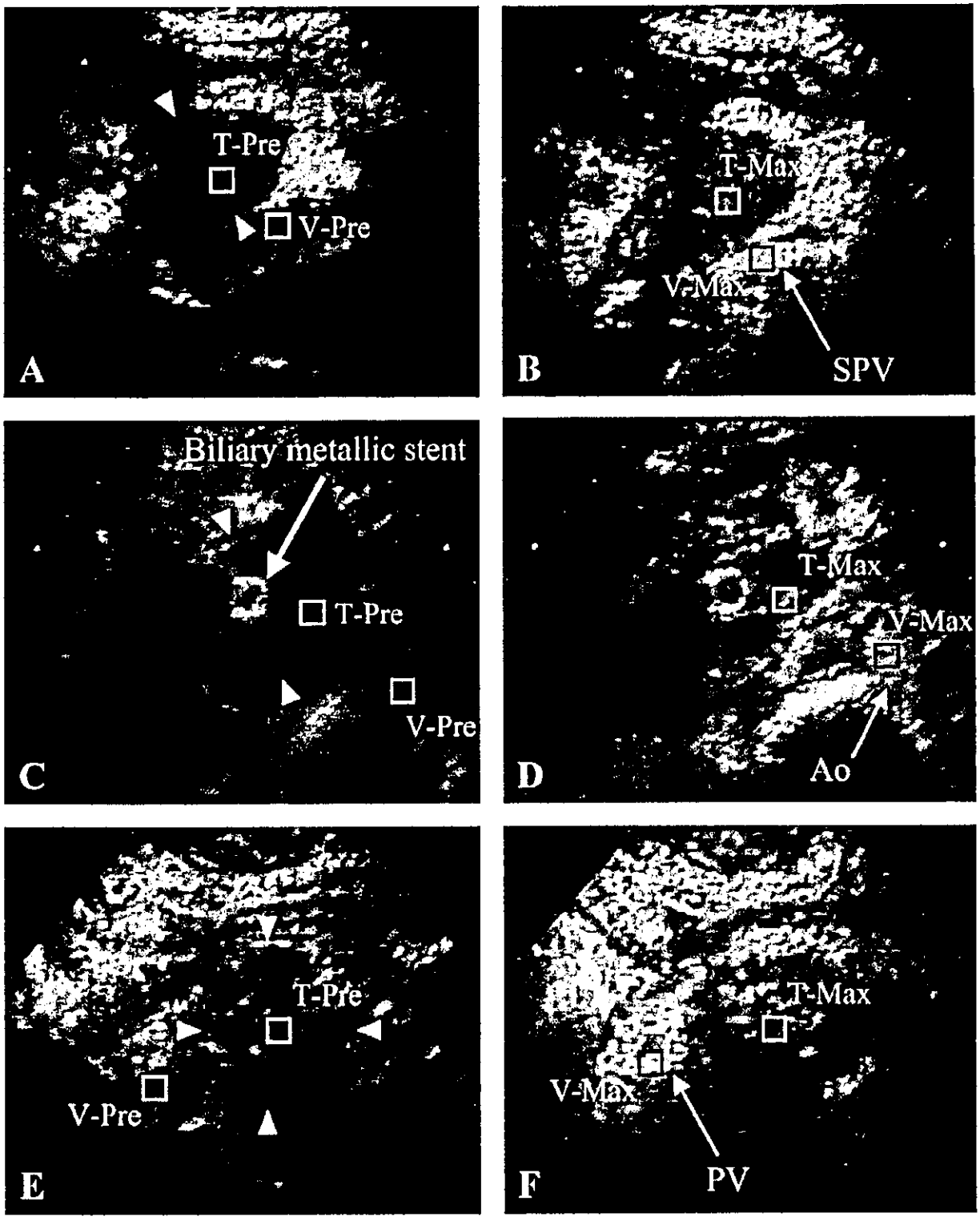
T-Pre
V-Pre
A
T-Max
V-Max
SPV
B
Biliary metallic stent
T-Pre
V-Pre
C
T-Max
V-Max
Ao
D
T-Pre
V-Pre
E
T-Max
V-Max
PV
F

FIGURE 1

a Microsoft Windows 98 environment (Microsoft Corporation, Redmond, WA), and the effect of enhancement by Levovist was quantified in Photoshop (version 5.0; Adobe Systems Corporation, San Jose, CA). Transverse images of the tumor that were obtained before enhancement and at maximal enhancement were selected. Five-millimeter square regions of interest (ROIs) containing 324 pixels were placed in the most enhanced portion within the tumor (avoiding large vessels involved in the tumor) and in the surrounding vessel (aorta, celiac trunk, superior mesenteric artery, portal vein, or splenic vein) on the US image obtained at maximal enhancement. The mean signal intensity in each of the ROIs, which represented tumor intensity (TI) or vessel intensity (VI), was measured by using the histogram function. TI and VI before enhancement also were measured in the ROIs corresponding to those at maximal enhancement, and then the relative tumor enhancement (RTE) to the surrounding vessel enhancement was calculated as the percentage of the increase in TI compared with the increase in VI between preenhancement and maximal enhancement with the following formula: RTE (%) = $(TI_{max} - TI_{pre}) \times 100/(VI_{max} - VI_{pre})$, in which max is maximal enhancement and pre is preenhancement (Fig. 1). That is, RTE was used as an index of tumor vascularity.

Chemotherapeutic Regimens

All patients were treated with either gemcitabine, S-1, or a combination of both. Twenty-eight patients received chemotherapy with gemcitabine (1000 mg/m^2), which was administered once weekly for 3 weeks followed by 1 week of rest. Four patients were treated with S-1 (80–120 mg/body), which was given twice daily for 28 days followed by 2 weeks of rest. Based on previous studies,[23,24] body surface area (BSA) was used to determine the dose of S-1 administered, as follows: BSA < 1.25 m^2, 80 mg; BSA = 1.25–1.5 m^2, 100 mg; BSA > 1.5 m^2, 120 mg. The remaining 3 patients received combination chemotherapy with gemcitabine (400–1000 mg/m^2) and S-1 (40–100 mg/body) conducted as a Phase I trial at our hospital. Dose escalation was performed in a stepwise manner in which the dose of one drug was escalated while the dose of the other drug was kept constant. Chemotherapy was continued until disease progression, death, or unacceptable toxicity.

Factors Analyzed

Along with RTE, 12 other variables were selected in the current study based on previous investigations[25–33] and our own clinical experience. All data were obtained just before the beginning of systemic chemotherapy. The variables were as follows: age, gender (male or female), primary tumor location (pancreatic head or pancreatic body and tail), primary tumor size, tumor status (metastatic or locally advanced), histologic grade (differentiated [Grade 1 and 2] or undifferentiated [Grade 3]), serum albumin level, serum lactate dehydrogenase (LDH) level, serum C-reactive protein (CRP) level, serum carcinoembryonic antigen (CEA) level, serum carbohydrate antigen 19-9 (CA 19-9) level, and prior biliary drainage (presence or absence). The size of the primary tumor was estimated carefully using enhanced CT and US studies.

Statistical Analysis

The time to progression (TTP) and survival were measured from the first day of chemotherapy to the date of progressive disease and death, respectively. Patients who did not die were censored at the time they were last known alive. The statistical significance of the correlation between RTE and clinicopathologic parameters was assessed with the Mann–Whitney U test, the Kruskal–Wallis test, or the Spearman rank correlation test. TTP and survival were estimated using the Kaplan–Meier method, and statistical comparisons were made with the log-rank test. Univariate and multivariate analyses were performed to determine significant variables related to prognosis with a Cox proportional hazards model. All P values were obtained with a 2-tailed statistical analysis, and P values < 0.05 were considered statistically significant. Statistical analyses

FIGURE 1. The patterns of tumor vascularity and the relative tumor enhancement in pancreatic carcinomas (A, C, and E) These ultrasonographic (US) images were obtained before administration of the contrast agent. (B, D, and F) These US images were captured at maximal enhancement after administration of the contrast agent. Five-millimeter square regions of interest (ROIs) are placed in the tumors and surrounding vessels on the unenhanced and enhanced US images. (A and B) Typical type of diffuse enhancement. (A) Poorly differentiated adenocarcinoma (arrowheads) measuring 2.9 cm in the pancreatic head. (B) Strong vascular signals are present throughout the lesion. The relative tumor enhancement in this image is 20.07% (C and D) Typical type of spotty enhancement. (C) Moderately differentiated adenocarcinoma (arrowheads) measuring 3.9 cm in the pancreatic head. (D) Mild vascular signals are observed in part of the tumor. The relative tumor enhancement in this image is 16.90%. (E and F) Typical type of no enhancement (E) Poorly differentiated adenocarcinoma (arrowheads) measuring 3.2 cm in the pancreatic body. Hyperechoic spots are seen before enhancement (F) Hardly any vascular signals are detected in the tumor. The relative tumor enhancement in this image is 9.56%. Squares indicate ROIs. T: tumor; V: vessel; Pre: preenhancement; Max: maximal enhancement; SPV: splenic vein; Ao: aorta; PV: portal vein.

were performed using the Statistical Package for Social Sciences (version 11.0; SPSS Inc., Chicago, IL).

RESULTS

Patient Follow-Up

Tumor assessment with US, CT, or magnetic resonance imaging (MRI) was performed every 4 weeks after the first course of systemic chemotherapy, and tumor response was evaluated according to World Health Organization criteria.[31] Five patients achieved an objective partial response. Objective stable disease (> 58 days) was documented in 12 patients, and objective progressive disease was documented in 18 patients. No patients achieved an objective complete response. The sites of disease recurrence and causes of death were investigated carefully. At the time of this analysis, the median follow-up for the 9 survivors was 183 days (range, 58–603 days), whereas the remaining 26 patients died between 28 days and 549 days (median, 123 days). All deaths occurred as a result of disease progression. There were no significant differences in TTP or survival among the groups that received different chemotherapeutic regimens.

Quantitative Analysis of Vascular Signal Assessed by Contrast-Enhanced US

After administration of the contrast agent, the increase in TI at maximal enhancement, compared with the TI before enhancement, ranged from 0.66 to 39.48 (median, 9.40; mean ± standard deviation, 11.47 ± 8.88). The intensity of the surrounding vessels also increased in all patients, with the elevation of intensity ranging from 26.55 to 106.27 (median, 55.09; mean ± standard deviation, 62.19 ± 21.95). In all 35 patients, the RTE to the surrounding vessel enhancement ranged from 1.12% to 53.23% (median, 16.50%; mean ± standard deviation, 18.07% ± 13.09%). None of the patients experienced complications such as allergic reactions or renal dysfunction.

We divided all patients into 2 groups (a group with vascular tumors and a group with avascular tumors) according to the cut-off value, which represented the median of the RTE in all pancreatic carcinomas (16.50%). Vascular tumors were defined as tumors in which the RTE value was > 16.5%, whereas avascular tumors were defined as tumors in which the RTE value was ≤ 16.5%.

Patterns of Tumor Vascularity Assessed by Contrast-Enhanced US

Three patterns of tumor vascularity were identified by contrast-enhanced US: diffuse enhancement (2 of 35 patients; 5.71%), spotty enhancement (18 of 35 patients; 51.43%), and no enhancement (15 of 35 patients; 42.86%) (Fig. 1). The RTE in the 3 patterns of tumor vascularity ranged from 20.07% to 50.75% (median, 35.41%; mean ± standard deviation, 35.41% ± 21.69%) in tumors with diffuse enhancement, from 12.25% to 53.23% (median, 20.16%; mean ± standard deviation, 24.50% ± 10.72%) in tumors with spotty enhancement, and from 1.12% to 23.08% (median 6.10%; mean ± standard deviation, 8.05% ± 6.25%) in tumors with no enhancement (Table 1). Among 17 vascular tumors, 2 tumors showed diffuse enhancement, 14 tumors showed spotty enhancement, and 1 tumor showed no enhancement; whereas, among 18 avascular tumors, 4 tumors showed spotty enhancement, and 14 tumors showed no enhancement.

Patient Characteristics and Relation between RTE and Clinicopathologic Factors

The patient characteristics are listed in Table 1. The median age was 61 years (range, 43–76 years), 21 patients were male, and 14 patients were female. The primary tumor location was the pancreatic head in 13 patients and the pancreatic body or tail in 22 patients. The primary tumor size ranged from 2.62 cm to 7.56 cm (median, 4.31 cm). Twenty-four patients had evidence of metastatic disease, and 11 patients had evidence of locally advanced disease. The histologic grade was differentiated in 23 patients and undifferentiated in 12 patients. Prior to chemotherapy, eight patients with obstructive jaundice underwent percutaneous transhepatic or endoscopic retrograde biliary drainage. RTE was associated closely with the patterns of tumor vascularity. There were no significant correlations between RTE and the other clinicopathologic factors.

Prognostic Value of Tumor Vascularity

The median TTP was 28 days for patients with vascular tumors and 110 days for patients with avascular tumors. The TTP curves are shown in Figure 2A. There was a significant difference in TTP between the 2 groups ($P = 0.0072$).

RTE ($P = 0.001$), primary tumor size ($P = 0.013$), tumor status ($P = 0.015$), histologic grade ($P = 0.026$), and serum LDH level ($P = 0.028$) all showed a significant relation with TTP in the univariate analysis. However, none of the other variables (age, gender, primary tumor location, serum albumin level, CRP level, CEA level, CA 19-9 level, and prior biliary drainage) reached a level of significance. Multivariate analysis using a Cox proportional hazards model showed that RTE ($P < 0.001$), primary tumor size ($P = 0.006$), tumor status ($P = 0.022$), and serum LDH level ($P = 0.007$) were significant independent factors influencing TTP (Table 2).

TABLE 1
Relation between Relative Tumor Enhancement and Clinicopathologic Factors

Characteristics	Relative tumor enhancement (%)		
	No. of patients	Median (range)	*P* value
Patterns of tumor vascularity			
Diffuse enhancement	2	35.41 (20.07–50.75)	< 0.001[a]
Spotty enhancement	18	20.16 (12.25–53.23)	
No enhancement	15	6.30 (1.12–23.08)	
Age (yrs)			
Median	61	rs 0.013	0.940[b]
Range	13–76		
Gender			
Male	21	16.23 (1.12–53.23)	0.522[c]
Female	14	16.60 (2.29–50.75)	
Tumor location			
Head	13	16.91 (1.28–42.97)	0.539[c]
Body-tail	22	15.64 (1.12–53.23)	
Tumor size (cm)			
Median	4.31	rs 0.333	0.050[b]
Range	2.62–7.56		
Tumor status			
Metastatic	24	15.51 (1.12–53.23)	0.749[c]
Locally advanced	11	18.37 (2.29–36.35)	
Histologic grade			
Differentiated	23	16.47 (1.28–36.35)	0.924[c]
Undifferentiated	12	18.29 (1.12–53.23)	
Albumin (g/dL)			
Median	3.90	rs 0.251	0.147[b]
Range	3.00–4.50		
LDH (U/L)			
Median	335	rs 0.242	0.161[b]
Range	205–861		
CRP (mg/dL)			
Median	1.93	rs 0.128	0.464[b]
Range	0.03–23.5		
CEA (ng/mL)			
Median	6.9	rs 0.051	0.770[b]
Range	1.0–650.0		
CA 19-9 (U/mL)			
Median	345	rs 0.192	0.269[b]
Range	11–425,000		
Prior biliary drainage			
Present	8	16.89 (12.24–42.97)	0.724[c]
Absent	27	16.30 (1.12–53.23)	
Anticancer agent			
Gemcitabine	28	16.48 (1.12–53.23)	0.949[c]
S-1	4	16.31 (9.56–29.08)	
Gemcitabine and S-1	3	16.91 (6.15–28.57)	

LDH, lactate dehydrogenase; CRP, C-reactive protein; CEA, carcinoembryonic antigen; CA 19-9, carbohydrate antigen 19-9; rs, Spearman rank correlation coefficient.
[a] Kruskal-Wallis test.
[b] Spearman rank correlation test.
[c] Mann-Whitney *U* test.

The median survival was 115 days for patients with vascular tumors and 267 days for patients with avascular tumors. The survival curves are shown in

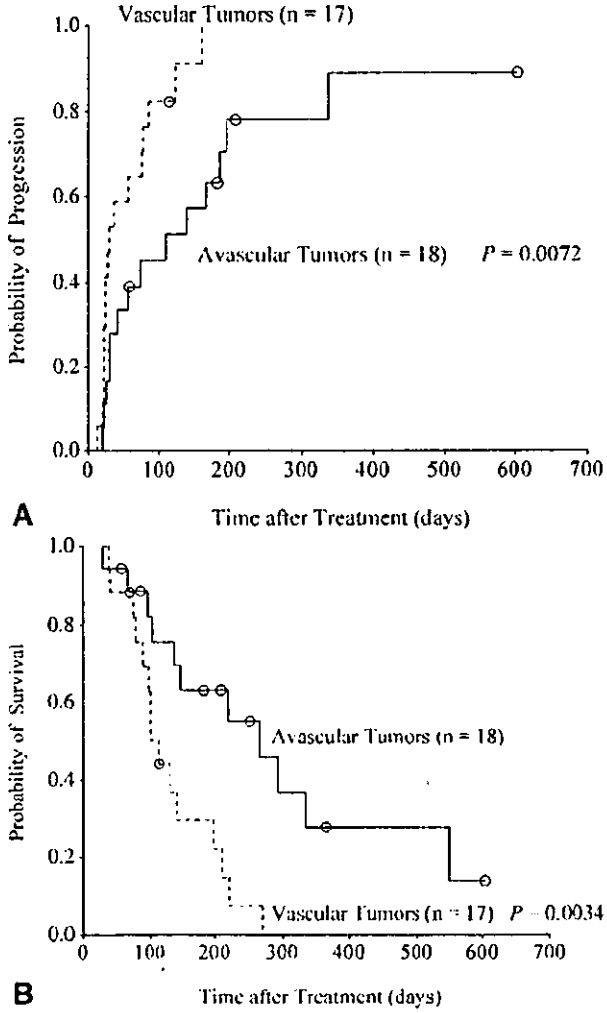

FIGURE 2. Progression and survival curves for 35 patients with nonresectable pancreatic carcinoma according to vascular and avascular tumors. The cut off value of relative tumor enhancement (RTE) is the median in all pancreatic carcinomas (16.5%). (A) Patients who had avascular tumors (RTE 16.5%) had a significantly lower incidence of disease progression compared with patients who had vascular tumors (RTE < 16.5%; *P* = 0.0072; log-rank test). (B) The survival of patients who had avascular tumors was significantly better compared with patients who had vascular tumors (*P* = 0.0034; log-rank test). Open circles indicate censored patients.

Figure 2B. The survival of patients with avascular tumors was significantly better ($P = 0.0034$).

RTE ($P = 0.003$), primary tumor size ($P = 0.002$), and serum levels of LDH ($P = 0.001$), CRP ($P = 0.001$), and CEA ($P = 0.025$), but not age, gender, primary tumor location, tumor status, histologic grade, serum albumin level, CA 19-9 level, or prior biliary drainage, showed a significant association with survival in the univariate analysis. Multivariate analysis using a Cox proportional hazards model showed that RTE (*P*

TABLE 2
Univariate and Multivariate Analyses of Prognostic Factors Associated with the Time to Disease Progression in Patients with Nonresectable Pancreatic Carcinoma

	Univariate analysis		Multivariate analysis	
Variables	HR (95% CI)	*P* value	HR (95% CI)	*P* value
Relative tumor enhancement	1.051 (1.021–1.081)	0.001	1.081 (1.035–1.128)	< 0.001
Age	1.028 (0.990–1.067)	0.149	1.027 (0.987–1.069)	0.190
Gender				
Male	0.987 (0.464–2.098)	0.973	0.646 (0.219–1.907)	0.423
Female				
Tumor location				
Head	1.046 (0.474–2.308)	0.912	1.108 (0.322–3.805)	0.871
Body-tail				
Primary tumor size	1.541 (1.085–2.189)	0.015	2.130 (1.242–3.653)	0.006
Tumor status				
Metastatic	2.916 (1.229–6.917)	0.015	4.847 (1.255–18.712)	0.022
Locally advanced				
Histologic grade				
Differentiated	0.421 (0.187–0.933)	0.026	0.992 (0.309–3.190)	0.890
Undifferentiated				
Albumin	0.750 (0.361–1.478)	0.382	0.365 (0.076–1.760)	0.208
LDH	1.003 (1.000–1.006)	0.028	1.007 (1.002–1.012)	0.007
CRP	1.061 (1.000–1.126)	0.050	0.842 (0.636–1.034)	0.100
CEA	1.001 (0.998–1.004)	0.429	1.000 (0.994–1.006)	0.978
Log of CA 19-9	1.121 (0.847–1.619)	0.439	0.647 (0.379–1.131)	0.127
Prior biliary drainage				
Present	0.693 (0.259–1.763)	0.411	0.134 (0.013–0.996)	0.050
Absent				

HR: hazard ratio; 95% CI: 95% confidence interval; LDH: lactate dehydrogenase; CRP: C-reactive protein; CEA: carcinoembryonic antigen; CA 19-9: carbohydrate antigen 19-9.

= 0.022), primary tumor size (P = 0.039), and serum LDH level (P = 0.001) had significant influence on survival as an independent factor (Table 3).

DISCUSSION

In the current study, TTP and survival were significantly longer in patients who had low tumor vascularity compared with patients who had high tumor vascularity. Furthermore, tumor vascularity was a significant independent factor that influenced TTP and survival along with primary tumor size and serum LDH level. Thus, we believe that contrast-enhanced US may be a valuable tool for prognostic evaluation and treatment planning in patients with nonresectable pancreatic carcinoma.

Pancreatic adenocarcinomas usually show hypovascular patterns on radiographic images obtained using contrast media, such as dynamic CT and angiography.[35,36] However, previous investigators have reported that adenocarcinoma itself showed some enhancement in a quantitative analysis of pancreatic enhancement during dual-phase helical CT.[37–39] Furthermore, several reports of pancreatic adenocarcinomas showed hypervascular findings.[10,11]

Contrast-enhanced US reportedly facilitates the detailed evaluation of tumor vascularity in hepatocellular carcinoma.[17,42] More recently, improved sensitivity to the contrast agent due to technical developments, such as harmonic imaging, has allowed better assessment of the vascularity of pancreatic tumors as well as hepatocellular carcinomas.[18–22,43] For example, Oshikawa et al.[18] reported that, after administration of the contrast agent, the change in TI of pancreatic carcinomas ranged from 0.1 dB to 18.6 dB. Nagase et al.[21] observed positive Doppler signals and intratumoral blood flow in 10.8% and 56.6%, respectively, of pancreatic ductal carcinomas. Ohshima et al.[11] found that the number of pancreatic carcinomas with definite vascular signal was greater than the number with almost no vascular signal (65% vs. 35%, respectively). Similarly, in the current study, we were able to detect tumor vascularity (diffuse and spotty enhancement) macroscopically in > 50% of the number of pancreatic carcinomas investigated with contrast-enhanced US (20 of 35 patients; 57.14%).

Oshikawa et al.[18] reported that, in 93% of tumors, any enhancement on dynamic sonography using Levovist was correlated closely with the grade of en-

TABLE 3
Univariate and Multivariate Analyses of Prognostic Factors Associated with Survival in Patients with Nonresectable Pancreatic Carcinoma

	Univariate analysis		Multivariate analysis	
Variables	HR (95% CI)	*P* value	HR (95% CI)	*P* value
Relative tumor enhancement	1.042 (1.014–1.072)	0.003	1.060 (1.008–1.113)	0.022
Age	1.019 (0.978–1.062)	0.364	1.005 (0.948–1.064)	0.874
Gender				
Male	1.054 (0.462–2.404)	0.900	1.207 (0.416–3.507)	0.729
Female				
Tumor location				
Head	2.103 (0.856–5.169)	0.105	1.915 (0.492–7.458)	0.349
Body-tail				
Primary tumor size	1.835 (1.242–2.709)	0.002	1.774 (1.030–3.054)	0.039
Tumor status				
Metastatic	2.061 (0.820–5.177)	0.124	1.648 (0.410–6.632)	0.482
Locally advanced				
Histologic grade				
Differentiated	0.625 (0.274–1.424)	0.264	0.967 (0.265–3.296)	0.957
Undifferentiated				
Albumin	0.556 (0.249–1.241)	0.152	0.441 (0.083–2.359)	0.339
LDH	1.005 (1.002–1.008)	0.001	1.010 (1.004–1.016)	0.001
CRP	1.146 (1.060–1.240)	0.001	0.970 (0.798–1.179)	0.759
CEA	1.004 (1.000–1.007)	0.025	1.000 (0.994–1.006)	0.994
Log of CA 19-9	1.260 (0.877–1.810)	0.211	0.565 (0.308–1.025)	0.064
Prior biliary drainage				
Present	1.389 (0.486–3.998)	0.541	0.472 (0.072–3.109)	0.434
Absent				

HR: hazard ratio, 95% CI: 95% confidence interval; LDH: lactate dehydrogenase; CRP: C-reactive protein; CEA: carcinoembryonic antigen; CA 19-9: carbohydrate antigen 19-9.

hancement on dynamic CT scans. Nagase et al.[21] examined tissue specimens obtained by surgical resection to assess the patterns of vascularity in pancreatic adenocarcinoma and showed that the ratio of patent vessels to total vessels was related to the degree of enhancement. Ohshima et al.[13] investigated the relation between contrast-enhanced Doppler signals and VEGF expression in pancreatic carcinomas and reported that VEGF expression was significantly higher in vascular tumors than in avascular tumors. In the current study, we could not compare tumor vascularity assessed by contrast-enhanced US with that assessed by histologic examination, because all lesions were nonresectable pancreatic carcinomas. However, reports indicate that contrast-enhanced US provides precise information on the vascularity of pancreatic carcinomas.

Angiogenesis is an important factor in the growth, progression, and metastasis of solid tumors, including pancreatic carcinomas.[8–11] Recently, it has been shown that the histologic assessment of intratumoral microvessel density and expression of angiogenic factors are important prognostic factors in pancreatic carcinomas.[12–14] However, all of those studies were conducted on patients who had undergone surgery, and no reports regarding the relation between angiogenesis and prognosis in patients with nonresectable pancreatic carcinoma have been published. The results of our current study provide evidence that contrast-enhanced US can be used to predict the outcome of patients with pancreatic carcinoma before treatment.

Patients with nonresectable pancreatic carcinomas have an especially poor prognosis and have many severe symptoms.[11] The analysis of prognostic factors before treatment may be helpful in selecting appropriate candidates for chemotherapy and determining treatment strategies. For example, patients who have a poor prognosis may be treated best with only supportive care because of their short survival. Alternatively, these patients may be treated with more aggressive treatment schedules, such as a more intensive multiagent chemotherapy or arterial infusion chemotherapy.[15] In the current study, we examined prognostic factors in patients with nonresectable pancreatic carcinoma. Among the variables investigated, RTE, primary tumor size, and serum LDH level were significant independent predictors of both TTP and survival, and tumor status was associated independently only with TTP in the multivariate analysis. Not only pri-

mary tumor size, serum LDH level, and tumor status but also age, histologic grade, and serum albumin, CRP, CEA, and CA 19-9 levels are well known prognostic factors in patients with resectable or nonresectable pancreatic carcinoma.[25-33] However, in the current study, multivariate analysis did not show that the latter six variables had significant predictive value for TTP or survival.

US examinations are essential to making a differential diagnosis of pancreatic masses, evaluating the extent of pancreatic lesions, and determining adequate treatments.[46,47] Furthermore, the results of our study lead us to conclude that the addition of contrast-enhanced US to conventional US may provide useful information more accurate than or equal to other prognostic factors in evaluating the malignant phenotype of pancreatic carcinomas or predicting chemotherapeutic effect. Contrast-enhanced US also has the advantage of not requiring exposure to X-rays and iodic contrast media, to which patients occasionally are allergic.[18] In fact, the contrast agent for US did not cause an allergic reaction and did not influence renal function in the current study.

However, contrast-enhanced US also has several flaws.[49,50] One major problem is that the method occasionally has limitations, such as a restricted image resolution of deep regions and poor visualization of the pancreas due to overlying abdominal gas. Another major problem is that contrast-enhanced US is not very precise in the evaluation of tumor vascularity, because it is dependent on the visual interpretations of the observer. In our past investigations, only 1 pancreatic lesion among > 100 pancreatic masses could not be detected using contrast-enhanced US. Moreover, the quantitative analysis of tumor vascularity enabled us to assess objectively the vascular information from pancreatic carcinomas. With regard to the quantitative analysis of tumor vascularity, two different types of analytic methods have been reported: One is the method for assessing the intensity of tumor enhancement, such as the contrast index[18,22] (contrast index = elevation of intensity in the tumor/elevation of intensity in the pancreatic parenchyma) and the RTE to the vessel enhancement used in this study, and the other is the method for assessing the area of tumor enhancement, such as the signal ratio[14] (signal ratio = vascular signal area/tumor area). However, the intensity of tumor enhancement was associated highly with the area of tumor enhancement according to the results from our study and from a previous report.[22] Oshikawa et al.[18] found that the contrast index was applicable only to patients in whom the pancreatic tumor and parenchyma can be scanned clearly in a single attempt. Therefore, in the current study on nonresectable, large pancreatic carcinomas, the RTE was more suitable for the quantitative analysis of tumor vascularity than the contrast index, because we could scan the tumor and surrounding vessels, but not the tumor and parenchyma, in a single attempt for all patients.

In conclusion, contrast-enhanced US ensures the assessability of tumor vascularity in pancreatic carcinomas. Patients who have avascular tumors have significantly longer TTP and survival compared with patients who have vascular tumors. Findings of contrast-enhanced US may be helpful in assessing the prognosis of patients with nonresectable pancreatic carcinoma who are receiving systemic chemotherapy.

REFERENCES

1. Burris HA 3rd, Moore MJ, Andersen J, et al. Improvements in survival and clinical benefit with gemcitabine as first-line therapy for patients with advanced pancreas cancer: a randomized trial. *J Clin Oncol.* 1997;15:2403–2413.
2. Rothenberg ML, Moore MJ, Cripps MC, et al. A Phase II trial of gemcitabine in patients with 5-FU-refractory pancreas cancer. *Ann Oncol.* 1996;7:347–353.
3. Hidalgo M, Castellano D, Paz-Ares L, et al. Phase I–II study of gemcitabine and fluorouracil as a continuous infusion in patients with pancreatic cancer. *J Clin Oncol.* 1999;17:585–592.
4. Ryan DP, Kulke MH, Fuchs CS, et al. A Phase II study of gemcitabine and docetaxel in patients with metastatic pancreatic carcinoma. *Cancer.* 2002;94:97–103.
5. Rocha Lima CM, Savarese D, Bruckner H, et al. Irinotecan plus gemcitabine induces both radiographic and CA 19-9 tumor marker responses in patients with previously untreated advanced pancreatic cancer. *J Clin Oncol.* 2002;20:1182–1191.
6. Louvet C, Andre T, Hedo G, et al. Gemcitabine combined with oxaliplatin in advanced pancreatic adenocarcinoma: final results of a GERCOR multicenter Phase II study. *J Clin Oncol.* 2002;20:1512–1518.
7. El-Rayes BF, Zalupski MM, Shields AF, et al. Phase II study of gemcitabine, cisplatin, and infusional fluorouracil in advanced pancreatic cancer. *J Clin Oncol.* 2003;21:2920–2925.
8. Folkman J. What is the evidence that tumors are angiogenesis dependent? *J Natl Cancer Inst.* 1990;82:4–6.
9. Liotta LA, Steeg PS, Stetler-Stevenson WG. Cancer metastasis and angiogenesis: an imbalance of positive and negative regulation. *Cell.* 1991;64:327–336.
10. Fidler IJ, Ellis LM. The implications of angiogenesis for the biology and therapy of cancer metastasis. *Cell.* 1994;79:185–188.
11. Shimoyama S, Gansauge F, Gansauge S, Negri G, Oohara T, Beger HG. Increased angiogenin expression in pancreatic cancer is related to cancer aggressiveness. *Cancer Res.* 1996;56:2703–2706.
12. Ikeda N, Adachi M, Taki T, et al. Prognostic significance of angiogenesis in human pancreatic cancer. *Br J Cancer.* 1999;79:1553–1563.
13. Seo Y, Baba H, Fukuda T, Takashima M, Sugimachi K. High expression of vascular endothelial growth factor is associated with liver metastasis and a poor prognosis for patients with ductal pancreatic adenocarcinoma. *Cancer.* 2000;88:2239–2245.

14. Fujioka S, Yoshida K, Yanagisawa S, Kawakami M, Aoki T, Yamazaki Y. Angiogenesis in pancreatic carcinoma: thymidine phosphorylase expression in stromal cells and intratumoral microvessel density as independent predictors of overall and relapse-free survival. *Cancer*. 2001;92:1788–1797.
15. Hosten N, Puls R, Lemke AJ, et al. Contrast-enhanced power Doppler sonography: improved detection of characteristic flow patterns in focal liver lesions. *J Clin Ultrasound*. 1999; 27:107–115.
16. Wilson SR, Burns PN, Muradali D, Wilson JA, Lai X. Harmonic hepatic US with microbubble contrast agent: initial experience showing improved characterization of hemangioma, hepatocellular carcinoma, and metastasis. *Radiology*. 2000;215:153–161.
17. Ding H, Kudo M, Onda H, Suetomi Y, Minami Y, Maekawa K. Hepatocellular carcinoma: depiction of tumor parenchymal flow with intermittent harmonic power Doppler US during the early arterial phase in dual-display mode. *Radiology*. 2001;220:349–356.
18. Oshikawa O, Tanaka S, Ioka T, Nakaizumi A, Hamada Y, Mitani T. Dynamic sonography of pancreatic tumors: comparison with dynamic CT. *AJR Am J Roentgenol*. 2002;178: 1133–1137.
19. Ozawa Y, Numata K, Tanaka K, et al. Contrast-enhanced sonography of small pancreatic mass lesions. *J Ultrasound Med*. 2002;21:983–991.
20. Takeda K, Goto H, Hirooka Y, et al. Contrast-enhanced transabdominal ultrasonography in the diagnosis of pancreatic mass lesions. *Acta Radiol*. 2003;44:103–106.
21. Nagase M, Furuse J, Ishii H, Yoshino M. Evaluation of contrast enhancement patterns in pancreatic tumors by coded harmonic sonographic imaging with a microbubble contrast agent. *J Ultrasound Med* 2003;22:789–795.
22. Kitano M, Kudo M, Maekawa K, et al. Dynamic imaging of pancreatic diseases by contrast enhanced coded phase inversion harmonic ultrasonography. *Gut*. 2004;53:854–859.
23. Ohtsu A, Baba H, Sakata Y, et al. Phase II study of S-1, a novel oral fluoropyrimidine derivative, in patients with metastatic colorectal carcinoma. *Br J Cancer*. 2000;83:141–145.
24. Hayashi K, Imaizumi T, Uchida K, Kuramochi H, Takasaki K. High response rates in patients with pancreatic cancer using the novel oral fluoropyrimidine S-1. *Oncol Rep*. 2002;9:1355–1361.
25. Kellokumpu-Lehtinen P, Huovinen R, Tuominen J. Pancreatic cancer. Evaluation of prognostic factors and treatment results. *Acta Oncol*. 1989;28:481–484.
26. Allison DC, Bose KK, Hruban RH, et al. Pancreatic cancer cell DNA content correlates with long-term survival after pancreatoduodenectomy. *Ann Surg*. 1991;214:648–656.
27. Geer RJ, Brennan MF. Prognostic indicators for survival after resection of pancreatic adenocarcinoma. *Am J Surg*. 1993; 165:68–73.
28. Lundin J, Roberts PJ, Kuusela P, Haglund C. The prognostic value of preoperative serum levels of CA 19-9 and CEA in patients with pancreatic cancer. *Br J Cancer*. 1994;69:515–519.
29. Yasue M, Sakamoto J, Teramukai S, et al. Prognostic values of preoperative and postoperative CEA and CA19-9 levels in pancreatic cancer. *Pancreas*. 1994;9:735–740.
30. Falconer JS, Fearon KCH, Ross JA, et al. Acute-phase protein response and survival duration of patients with pancreatic cancer. *Cancer*. 1995;75:2077–2082.
31. Ueno H, Okada S, Okusaka T, Ikeda M. Prognostic factors in patients with metastatic pancreatic adenocarcinoma receiving systemic chemotherapy. *Oncology*. 2000;59:296–301.
32. Ikeda M, Okada S, Tokuuye K, Ueno H, Okusaka T. Prognostic factors in patients with locally advanced pancreatic carcinoma receiving chemoradiotherapy. *Cancer*. 2001;91: 490–495.
33. Tas F, Aykan F, Alici S, Kaytan E, Aydiner A, Topuz E. Prognostic factors in pancreatic carcinoma: Serum LDH levels predict survival in metastatic disease. *Am J Clin Oncol*. 2001;24:547–550.
34. World Health Organization. WHO handbook for reporting results of cancer treatment. Geneva: World Health Organization, 1979.
35. Ghosh BC, Mojab K, Esfahani F, Moss GS, Das Gupta TK. Role of angiography in the diagnosis of pancreatic neoplasms. *Am J Surg*. 1979;138:675–677.
36. Hosoki T. Dynamic CT of pancreatic tumors. *AJR Am J Roentgenol*. 1983;140:959–965.
37. Lu DSK, Vedantham S, Krasny RM, Kadell B, Berger WL, Reber HA. Two-phase helical CT for pancreatic tumors: pancreatic versus hepatic phase enhancement of tumor, pancreas, and vascular structures. *Radiology*. 1996;199:697–701.
38. Graf O, Boland GW, Warshaw AL, Fernandez-del-Castillo C, Hahn PF, Mueller PR. Arterial versus portal venous helical CT for revealing pancreatic adenocarcinoma: conspicuity of tumor and critical vascular anatomy. *AJR Am J Roentgenol*. 1997;169:119–123.
39. Boland GW, O'Malley ME, Saez M, Fernandez-del-Castillo C, Warshaw AL, Mueller PR. Pancreatic-phase versus portal vein-phase helical CT of the pancreas: optimal temporal window for evaluation of pancreatic adenocarcinoma. *AJR Am J Roentgenol*. 1999;172:605–608.
40. Park CM, Cha IH, Choi SY, Kim HK. Hyperdense enhancement of pancreatic adenocarcinoma on spiral CT: two case reports. *Clin Imaging*. 1999;23:187–189.
41. Becker D, Strobel D, Bernatik T, Hahn EG. Echo-enhanced color- and power-Doppler EUS for the discrimination between focal pancreatitis and pancreatic carcinoma. *Gastrointest Endosc*. 2001;53:784–789.
42. Choi BI, Kim AY, Lee JY, et al. Hepatocellular carcinoma: contrast enhancement with Levovist. *J Ultrasound Med*. 2002;21:77–84.
43. Ohshima T, Yamaguchi T, Ishihara T, et al. Evaluation of blood flow in pancreatic ductal carcinoma using contrast-enhanced, wide-band Doppler ultrasonography: correlation with tumor characteristics and vascular endothelial growth factor. *Pancreas*. 2004;28:335–343.
44. Kalser MH, Barkin J, MacIntyre JM. Pancreatic cancer. Assessment of prognosis by clinical presentation. *Cancer*. 1985;56:397–402.
45. Homma H, Doi T, Mezawa S, et al. A novel arterial infusion chemotherapy for the treatment of patients with advanced pancreatic carcinoma after vascular supply distribution via superselective embolization. *Cancer*. 2000;89:303–313.
46. Taylor KJ, Rosenfield AT. Grey-scale ultrasonography in the differential diagnosis of jaundice. *Arch Surg*. 1977;112:820–825.
47. Pollock D, Taylor KJ. Ultrasound scanning in patients with clinical suspicion of pancreatic cancer: a retrospective study. *Cancer*. 1981;47:1662–1665.
48. Otis S, Rush M, Boyajian R. Contrast-enhanced transcranial imaging. Results of an American phase-two study. *Stroke*. 1995;26:203–209.
49. Van Dyke JA, Stanley RJ, Berland LL. Pancreatic imaging. *Ann Intern Med*. 1985;102:212–217.
50. Balthazar EJ, Chako AC. Computed tomography of pancreatic masses. *Am J Gastroenterol*. 1990;85:343–349.

ORIGINAL ARTICLE

Differential diagnosis of pancreatic cancer and focal pancreatitis by using EUS-guided FNA

Kuniyuki Takahashi, MD, Kenji Yamao, MD, Kenji Okubo, MD, Akira Sawaki, MD, Nobumasa Mizuno, MD, Reiko Ashida, MD, Takashi Koshikawa, MD, Yuji Ueyama, CT, Kunio Kasugai, MD, Satoshi Hase, MD, Shinichi Kakumu, MD

Nagoya, Japan

Background: Despite advances in diagnostic imaging techniques, the differentiation between pancreatic cancer and focal pancreatitis remains difficult. This study evaluated the effectiveness of EUS-guided FNA in the differential diagnosis between pancreatic cancer and focal pancreatitis, with particular reference to detection of the K-*ras* point mutation.

Methods: The study included 62 consecutive patients with pancreatic ductal cancer and 15 patients with focal pancreatitis demonstrated as a pancreatic mass lesion by EUS.

Results: Sensitivity, specificity, overall accuracy, positive predictive value, and negative predictive value of cytopathologic diagnosis were 82%, 100%, 86%, 100%, and 58%, respectively. Sensitivity, specificity, overall accuracy, positive predictive value, and negative predictive value of histopathologic diagnosis were 44%, 100%, 55%, 100%, and 32%, respectively. The K-*ras* point mutation was found in 74% of pancreatic cancers and 0% of focal pancreatitis lesions. No complication of EUS-guided FNA was observed.

Conclusions: EUS-guided FNA is useful for the differential diagnosis of pancreatic mass lesions caused by pancreatic cancer and focal pancreatitis. Analysis for the K-*ras* point mutation in specimens obtained by EUS-guided FNA may enhance diagnostic accuracy in indeterminate cases. (Gastrointest Endosc 2005;61:76-9.)

Despite advances in diagnostic imaging techniques, the differentiation of pancreatic cancer from focal pancreatitis remains problematic.[1-4] Indeed, there are cases in which focal pancreatitis was misdiagnosed as pancreatic cancer or when surgery was performed because pancreatic cancer could not be absolutely ruled out. EUS-guided FNA (EUS-FNA) has been used for the differential diagnosis of pancreatic masses, staging of pancreatic cancer, and histopathologic confirmation of the diagnosis of pancreatic cancer before radiotherapy and/or chemotherapy.[5-9] However, there are few studies of K-*ras* point mutation analysis for pancreatic tissue obtained by EUS-FNA.[5,6] The present study examined the effectiveness of EUS-FNA, specifically, cytopathologic and histopathologic evaluation, and analysis of K-*ras* point mutation, for specimens obtained by EUS-FNA in the differential diagnosis of pancreatic cancer vs. focal pancreatitis.

0016-5107/2005/$30.00 + 0

PII: S0016-5107(04)02224-2

PATIENTS AND METHODS

The study included 62 patients with a diagnosis of pancreatic ductal cancer and 15 patients with focal pancreatitis (total 77 patients) who underwent EUS-FNA between August 1998 and April 2003 for whom the results of cytopathologic and histopathologic evaluation, and K-*ras* point mutation analysis could be obtained. Final diagnoses were confirmed by evaluation of surgical resection specimens in 8 patients (pancreatic cancer 6, focal pancreatitis 2) and by clinical follow-up of 9 months or longer for the remainder of the patients (pancreatic cancer 56, focal pancreatitis 13).

EUS-FNA was performed as previously described,[1,5,8] by using a 7.5 MHz, convex linear-array echoendoscope (GF-UCT240; Olympus Optical Co., Ltd., Tokyo, Japan) and a 22-gauge needle (NA-10J-1 or NA-11J-KB; Olympus). Aspirated material was divided into 3 parts: one for cytopathologic evaluation, another for histopathologic assessment, and the last for K-*ras* point mutation analysis.

For all 77 patients, aspirated material was immediately evaluated by a cytopathologist or a cytotechnician for rapid cytopathologic diagnosis.[5,8] Aspirated material was

ORIGINAL ARTICLE

Differential diagnosis of pancreatic cancer and focal pancreatitis by using EUS-guided FNA

Kuniyuki Takahashi, MD, Kenji Yamao, MD, Kenji Okubo, MD, Akira Sawaki, MD, Nobumasa Mizuno, MD, Reiko Ashida, MD, Takashi Koshikawa, MD, Yuji Ueyama, CT, Kunio Kasugai, MD, Satoshi Hase, MD, Shinichi Kakumu, MD

Nagoya, Japan

Background: Despite advances in diagnostic imaging techniques, the differentiation between pancreatic cancer and focal pancreatitis remains difficult. This study evaluated the effectiveness of EUS-guided FNA in the differential diagnosis between pancreatic cancer and focal pancreatitis, with particular reference to detection of the K-*ras* point mutation.

Methods: The study included 62 consecutive patients with pancreatic ductal cancer and 15 patients with focal pancreatitis demonstrated as a pancreatic mass lesion by EUS.

Results: Sensitivity, specificity, overall accuracy, positive predictive value, and negative predictive value of cytopathologic diagnosis were 82%, 100%, 86%, 100%, and 58%, respectively. Sensitivity, specificity, overall accuracy, positive predictive value, and negative predictive value of histopathologic diagnosis were 44%, 100%, 55%, 100%, and 32%, respectively. The K-*ras* point mutation was found in 74% of pancreatic cancers and 0% of focal pancreatitis lesions. No complication of EUS-guided FNA was observed.

Conclusions: EUS-guided FNA is useful for the differential diagnosis of pancreatic mass lesions caused by pancreatic cancer and focal pancreatitis. Analysis for the K-*ras* point mutation in specimens obtained by EUS-guided FNA may enhance diagnostic accuracy in indeterminate cases. (Gastrointest Endosc 2005;61:76-9.)

Despite advances in diagnostic imaging techniques, the differentiation of pancreatic cancer from focal pancreatitis remains problematic.[1-4] Indeed, there are cases in which focal pancreatitis was misdiagnosed as pancreatic cancer or when surgery was performed because pancreatic cancer could not be absolutely ruled out. EUS-guided FNA (EUS-FNA) has been used for the differential diagnosis of pancreatic masses, staging of pancreatic cancer, and histopathologic confirmation of the diagnosis of pancreatic cancer before radiotherapy and/or chemotherapy.[5-9] However, there are few studies of K-*ras* point mutation analysis for pancreatic tissue obtained by EUS-FNA.[5,6] The present study examined the effectiveness of EUS-FNA, specifically, cytopathologic and histopathologic evaluation, and analysis of K-*ras* point mutation, for specimens obtained by EUS-FNA in the differential diagnosis of pancreatic cancer vs. focal pancreatitis.

0016-5107/2005/$30.00 + 0

PII: S0016-5107(04)02224-2

PATIENTS AND METHODS

The study included 62 patients with a diagnosis of pancreatic ductal cancer and 15 patients with focal pancreatitis (total 77 patients) who underwent EUS-FNA between August 1998 and April 2003 for whom the results of cytopathologic and histopathologic evaluation, and K-*ras* point mutation analysis could be obtained. Final diagnoses were confirmed by evaluation of surgical resection specimens in 8 patients (pancreatic cancer 6, focal pancreatitis 2) and by clinical follow-up of 9 months or longer for the remainder of the patients (pancreatic cancer 56, focal pancreatitis 13).

EUS-FNA was performed as previously described,[1,5,8] by using a 7.5 MHz, convex linear-array echoendoscope (GF-UCT240; Olympus Optical Co., Ltd., Tokyo, Japan) and a 22-gauge needle (NA-10J-1 or NA-11J-KB; Olympus). Aspirated material was divided into 3 parts: one for cytopathologic evaluation, another for histopathologic assessment, and the last for K-*ras* point mutation analysis.

For all 77 patients, aspirated material was immediately evaluated by a cytopathologist or a cytotechnician for rapid cytopathologic diagnosis.[5,8] Aspirated material was

TABLE 1. Clinical characteristics of patients undergoing EUS-FNA

	Pancreatic cancer	Focal pancreatitis
No. patients (M/F)	62 (40/22)	15 (10/5)
Mean age y (range)	60 (35-79)	60 (50-71)
Mean number of needle passes (range)	2.3 (1-4)	2.4 (1-4)
Location (% head)	84%	85%
Mean size of mass, mm (range)	36 (16-80)	31 (21-40)

Capsule Summary

What is already known on this topic

- It is difficult to differentiate between pancreatic cancer and focal pancreatitis.
- EUS-guided FNA biopsy (EUS-FNA) is very useful in the differential diagnosis of pancreatic lesions and in the diagnosis and staging of pancreatic cancer.

What this study adds to our knowledge

- K-*ras* point mutation is not seen in focal pancreatitis.
- Testing specimens obtained by EUS-FNAB for K-*ras* mutation by PCR improves the sensitivity for the diagnosis of pancreatic cancer by about 10%.

TABLE 2. Diagnostic accuracy for cytopathologic evaluation of specimens obtained by EUS-FNA

	Pancreatic cancer	Focal pancreatitis
No malignancy	4 (7%)	15 (100%)
Suspicion of malignancy	7 (11%)	0
Malignancy	51 (82%)	0
Total	62	15

TABLE 3. Diagnostic accuracy for histopathologic evaluation of specimens obtained by EUS-FNA

	Pancreatic cancer	Focal pancreatitis
Insufficient material	7 (11%)	1 (7%)
No malignancy	11 (18%)	14 (93%)
Atypical epithelium	5 (8%)	0
Suspicious of malignancy	15 (24%)	0
Malignancy	24 (39%)	0
Total	62	15

later stained by using Papanicolaou's method. For histopathologic diagnosis, material aspirated with a 22-gauge needle was directly fixed in formalin in a specimen bottle and then was embedded in paraffin. Sections then were stained (H&E). The existence of a point mutation at codon 12 in the K-*ras* gene was examined in all 77 cases by incubating the collected specimen in 10 mL of saline solution at 4°C and then by analyzing the mixture by polymerase chain reaction–single-strand conformation polymorphism (PCR-SSCP) and direct sequencing.[10-14]

Informed consent was obtained from all patients. The study was approved by the institutional review board of our hospital.

RESULTS

There was no significant difference between the patient groups with respect to age, gender, number of needle passes, and location or size of the mass (Table 1).

Cytopathologic diagnosis

Of the 62 cases of pancreatic cancer, cytopathologic assessment of the aspirated material diagnosed 4 as non-malignant, 7 as suspicious for malignancy, and 51 as malignant (Table 2). The sensitivity was 82% (51/62: 95% confidence interval [CI][73%, 92%]). Of the 15 cases of focal pancreatitis, all were diagnosed as non-malignant (Table 2). The specificity was 100% (15/15: 95% CI[78%, 100%]). There was no false-positive diagnosis. The overall accuracy, positive predictive value (PPV), and negative predictive value (NPV) were 86%: 95% CI[78%, 94%]), 100%, and 58%, respectively.

Histopathologic diagnosis

The aspirated specimen was insufficient for histopathologic diagnosis in 7 of the 62 cases of pancreatic cancer: these cases were excluded from the calculations for sensitivity, specificity, overall accuracy, PPV, and NPV. Of the remaining 55 cases of pancreatic cancer, no findings indicative of malignancy were detected in 11, atypical epithelium was noted in 5, findings that raised a suspicion of cancer were present in 15, and malignancy was diagnosed in 24 cases (Table 3). The sensitivity was 44% (24/55: 95% CI[31%, 57%]) (Table 3). The aspirated specimen was insufficient for histopathologic assessment in one of the 15 cases of focal pancreatitis. No evidence of malignancy was noted in the remaining 14 cases (Table 3). The specificity was 100% (14/14: 95% CI[78%, 100%]). The overall accuracy, PPV, and NPV were 55% (38/69: 95% CI[43%, 67%]), 100%, and 32%, respectively.

TABLE 4. Detection of K-*ras* point mutation in specimens from pancreatic mass lesions obtained by EUS-FNA

K-*ras* point mutation	Pancreatic cancer	Focal pancreatitis
Positive	46 (74%)	0
Negative	16 (26%)	15 (100%)
Total	62	15

TABLE 5. Relationship between cytopathologic evaluation and K-*ras* point mutation in specimens of pancreatic cancer obtained by EUS-FNA

	Cytology	K-*ras* point mutation positive
No malignancy	4	2 (50%)
Suspicion of malignancy	7	5 (71%)
Malignancy	51	39 (76%)
Total	62	46

Detection of K-*ras* codon 12-point mutation

A point mutation was detected in 74% (46/62: 95% CI[62%, 85%]) of the 62 cases of pancreatic cancer (Table 4). Of the 46 cases in which the K-*ras* point mutation was detected, the mutation was at GAT in 22 (35.4%), at GTT in 14 (22.5%), at CGT in 9 (14.5%), and at TGT in one case (0.2%). No mutation was found in the remaining 16 cases (25.8%) of pancreatic cancer. However, no K-*ras* point mutation was observed in any of the 15 cases of focal pancreatitis. When cases with a positive K-*ras* mutation were assumed to be malignant and those negative for the K-*ras* mutation were assumed to be benign, the diagnostic accuracy was 79% (61/77: 95% CI[69%, 88%]).

Relationship between histopathologic and cytopathologic evaluation, and detection of K-*ras* codon 12-point mutation in pancreatic cancer

With respect to cytopathologic diagnosis, the K-*ras* point mutation was found in 50% (2/4) of cases, with a result of no malignancy; in 71% (5/7) of cases in which malignancy was suspected; and in 76% (39/51) of cases in which malignancy was diagnosed (Table 5). With respect to histopathologic diagnosis, the K-*ras* point mutation was detected in 43% (3/7) of cases with a result of insufficient material, in 64% (7/11) of those with no malignancy, in 80% (4/5) of cases with a finding of atypia, in 80% (12/15) of cases in which malignancy was suspected, and in 83% (20/24) of cases in which malignancy was diagnosed (Table 6).

If it is assumed that at least one positive diagnosis of cancer (cytopathologic and/or histopathologic and/or detection of K-*ras* codon 12-point mutation) was accurate, the sensitivity of EUS-FNA improved to 94% (58/62) (Table 7).

TABLE 6. Relationship between histopathologic evaluation and K-*ras* point mutation in specimens of pancreatic cancer obtained by EUS-FNA

	Histology	K-*ras* point mutation positive
Insufficient material	7	3 (43%)
No malignancy	11	7 (64%)
Atypical	5	4 (80%)
Suspicion of malignancy	15	12 (80%)
Malignancy material	24	20 (83%)
Total	62	46

TABLE 7. Sensitivity for pancreatic cancer for combined cytopathologic evaluation, histopathologic evaluation, and K-*ras* point mutation

	Pancreatic cancer
Cytology positive	51 (82%)
Cytology positive and/or histology positive	52 (84%)
Cytology positive and/or histology positive and/or K-*ras* mutation positive	58 (94%)
Total	62

Complications

No complication associated with EUS-FNA was observed in any of the 77 patients.

DISCUSSION

Compared with the rest of the GI tract, a nonoperative biopsy specimen of the pancreas is difficult to obtain. Nevertheless, there have been many studies of methods for obtaining a histopathologic or a cytopathologic diagnosis, including US- and CT-guided percutaneous biopsy, transpapillary pancreatic duct biopsy, and cytologic evaluation of pancreatic juice obtained at ERCP.[1,5,15] With the development of EUS-FNA, however, the ability to accurately diagnose pancreatic malignancy has greatly improved.[1,5,15] The ability to visualize small lesions with EUS is excellent, and, unlike other methods, the entire pancreas is readily imaged.[1,15,16] Thus, EUS-FNA is considered to be the best of the available methods for obtaining tissue samples from the pancreas. In studies that include a relatively large number of patients, the sensitivity,

the specificity, and the overall accuracy of EUS-FNA for pancreatic cancer are 80% to 92%, 100%, and 85% to 95%, respectively.[1,5] These results are almost identical to those of the present study. Thus, differentiation between benign and malignant pancreatic lesions has been considerably improved because of the development and the improvement of echoendoscopes and because of the introduction of rapid staining techniques that allow immediate assessment of aspirated material by a cytopathologist or a cytotechnician. However, there is still a relatively large number of cases in which the differential diagnosis of pancreatic mass lesions remains problematic.[16,17]

Various genetic abnormalities have been demonstrated in pancreatic cancer.[4,18] The most frequent is the K-*ras* codon 12-point mutation. This mutation is detected in 75% to 100% of pancreatic ductal cancers,[18,19] whereas it is rarely present in mass-forming pancreatitis.[4] Thus, it was hypothesized by us that detection of the K-*ras* point mutation by using tissue obtained by EUS-FNA would be an ideal method for clarification of the presence of malignancy.

The K-*ras* codon 12-point mutation was detected in 74% of the cases of pancreatic cancer in the present study, and it was not observed in any case of focal pancreatitis. This rate of detection is slightly lower than that found in other studies that used pancreatic resection specimens. This is possibly attributable to two factors: (1) heterogeneity in gene mutation in pancreatic cancer and (2) a sufficient specimen of pancreatic cancer could not be collected by EUS-FNA. However, the sensitivity for the diagnosis of pancreatic cancer improved markedly, from 82% to 94%, in cases of pancreatic cancer when the presence of the K-*ras* mutation was taken into consideration. Thus, the detection of the K-*ras* codon 12-point mutation by using specimens obtained by EUS-FNA proved to be useful in differentiating pancreatic cancer and focal pancreatitis.

In conclusion, the present study found that the K-*ras* mutation can be detected in specimens obtained by EUS-FNA. With the addition of K-*ras* mutation analysis, EUS-FNA was highly accurate for the differentiation of benign vs. malignant pancreatic mass lesions. The results of the current study suggest that K-*ras* mutation analysis can provide important information with regard to the diagnosis of pancreatic masses. Further prospective trials are required to confirm the efficacy of this technique.

REFERENCES

1. Harewood GC, Wiersema MJ. Endosonography-guided fine needle aspiration biopsy in the evaluation of pancreatic mass. Am J Gastroenterol 2002;97:1386-91.
2. Muller MF, Meyenber C, Bertschinger P, Schaer R, Marincek B. Pancreatic tumors: evaluation with endoscopic US, CT, and MR imaging. Radiology 1994;190:745-51.
3. Howard TJ, Chin AC, Streib EW, Kopecky KK, Wiebke EA. Value of helical computed tomography, angiography, and endoscopic ultrasound in determining resectability of periampullary carcinoma. Am J Surg 1997;174:237-41.
4. Matsubayashi H, Watanabe H, Ajioka Y, Nishikura K, Yamano M, Seki T. Different amounts of K-*ras* mutant epithelial cells in pancreatic carcinoma and mass-forming pancreatitis. Pancreas 2000;21:77-85.
5. Tada M, Komatsu Y, Kawabe T, Sasahira N, Isayama H, Toda N. Quantitative analysis of K-*ras* gene mutation in pancreatic tissue obtained by endoscopic ultrasonography-guided fine needle aspiration: clinical utility diagnosis of pancreatic tumor. Am J Gastroenterol 2002;97:1386-90.
6. Villanueva A, Reyes G, Cuatrecasas M, Martinez A, Erill N, Lerma E. Diagnostic utility of K-*ras* mutations in fine-needle aspirates of pancreatic masses. Gastroenterology 1996;110:1587-94.
7. Wiersema MJ, Vilmann P, Giovannini M, Chang KJ, Wiersema LM. Endosonography-guided fine-needle aspiration biopsy: diagnostic accuracy and complication assessment. Gastroenterology 1997;112:1087-95.
8. Chang KJ, Nguyen P, Erickson RA, Durbin TE, Katz KD. The clinical utility of endoscopic ultrasound-guided fine-needle aspiration in the diagnosis and staging of pancreatic carcinoma. Gastrointest Endosc 1997;45:387-93.
9. Erickson RA, Sayage-Rabie L, Avots-Avotins A. Clinical utility of endoscopic ultrasound-guided fine needle aspiration. Acta Cytol 1997;41: 1647-53.
10. Owens DM, Smart RC. A multihit, multistage model of chemical carcinogenesis. Carcinogenesis 1999;20:1837-44.
11. Huber KR, Bittner J, Bauer K, Trumper L, Sek A, Sebesta C. Restriction digest PCR (RD-PCR) for the analysis of gene mutations. Application to Ki-ras. Clin Chem Lab Med 1998;36:593-5.
12. Kopreski MS, Benko FA, Kwee C, Leitzel KE, Eskander E, Lipton A. Detection of mutant K-*ras* DNA in plasma or serum of patient with colorectal cancer. Br J Cancer 1997;76:1293-9.
13. Ronai Z, Minoamoto T. Quantitaive enriched PCR(QEPCR), a highly sensitive method for detection of K-*ras* oncogene mutation. Hum Mutat 1997;10:322-5.
14. Banerjee SK, Makdisi WF, Weston AP, Campbell DR. A two-step enriched-nested PCR technique enhances sensitivity for detection of codon 12 K-*ras* mutations in pancreatic adenocarcinoma. Pancreas 1997;15:16-24.
15. Okai T, Watanabe H, Yamaguchi Y, Mouri I, Motoo Y, Sawabu N. EUS and K-*ras* analysis of pure pancreatic juice collected via a duodenoscope after secretin stimulation for diagnosis of pancreatic mass lesion: a prospective study. Gastrointest Endosc 1999;50:797-803.
16. Mallery JS, Centeno BA, Hahn PF, Chang Y, Warshaw AL, Brugge WR. Pancreatic tissue sampling guided by EUS, CT/US, and surgery: a comparison of sensitivity and specificity. Gastrointest Endosc 2002; 56:218-24.
17. Eloubeidi MA, Jhala D, Chhieng DC, Chen VK, Eltoum I, Vicker S. Yield of endoscopic ultrasound-guided fine-needle aspiration biopsy in patients with suspected pancreatic carcinoma. Cancer 2003;99:285-92.
18. Berrozpe G, Schaeffer J, Peinado MA, Real FX, Perucho M. Comparative analysis of mutation in p53 and K-*ras* genes in pancreatic cancer. Int J Cancer 1994;58:185-91.
19. Tada M, Omata M, Ohto M. Clinical application of *ras* gene mutation for diagnosis of pancreatic adenocarcinoma. Gastroenterology 1991; 100:233-8.

Received February 17, 2004. For revision April 28, 2004. Accepted September 2, 2004.

Current affiliations: Department of Gastroenterology, Aichi Medical University School of Medicine, Aichi-gun, Japan, Departments of Gastroenterology and Pathology/Genetics, Aichi Cancer Center Hospital, Nagoya, Japan.

Reprint requests: Kenji Yamao, MD, Department of Gastroenterology, Aichi Cancer Center Hospital, 1-1 Kanokoden, Chikusa-ku, Nagoya 464-0021, Japan.

Cdx2 expression in pancreatic tumors: Relationship with prognosis of invasive ductal carcinomas

KAKUYA MATSUMOTO[1,2,4,*], TSUTOMU MIZOSHITA[1,*], TETSUYA TSUKAMOTO[1], NAOTAKA OGASAWARA[1], AKIHIRO HIRATA[1], YASUHIRO SHIMIZU[3], MASAKAZU HANEDA[4], KENJI YAMAO[2] and MASAE TATEMATSU[1]

[1]Division of Oncological Pathology, Aichi Cancer Center Research Institute, 1-1 Kanokoden, Chikusa-ku, Nagoya 464-8681; Departments of [2]Gastroenterology and [3]Gastroenterological Surgery, Aichi Cancer Center Hospital, 1-1 Kanokoden Chikusa-ku, Nagoya 464-8681; [4]Second Department of Internal Medicine, Asahikawa Medical College, 1-1-1 Higashi 2-jo, Midorigaoka, Asahikawa 078-8510, Japan

Received July 26, 2004; Accepted September 3, 2004

Abstract. We have previously reported that *Caudal*-related homeobox gene 2 (Cdx2) is a useful prognostic intestinal phenotypic marker for advanced gastric cancers. In this study, we examined Cdx2 expression and phenotype in pancreatic tumors. We evaluated 19 mucinous cystic tumors (MCTs), 17 intraductal papillary-mucinous tumors (IPMTs), and 41 invasive ductal carcinomas (IDCs) with regard to their gastrointestinal phenotype. The expression of Cdx2 was also assessed immunohistochemically. The lesions were phenotypically divided into 39 gastric (G type), 29 gastric and intestinal mixed (GI type), 3 intestinal (I type), and 6 null (N type) types, independent of the histopathological type. Most of the pancreatic tumors were thus judged to be the positive for gastric phenotypic members. Cdx2 nuclear staining demonstrated a close relation to the intestinal phenotypic expression in all three types (MCTs, IPMTs, and IDCs; $p<0.05$). In IDCs, Kaplan-Meier analysis of Cdx2 expression showed the Cdx2-positive group to have a significantly better outcome than their negative counterparts ($p=0.015$). In conclusion, our data suggest that Cdx2 might be necessary for intestinal phenotypic expression even in pancreatic tumor cells. In addition, Cdx2 expression in IDCs may be a novel prognostic marker for patient survival.

Introduction

It is well known that pancreatic tumors show gastrointestinal phenotypic expression with mucin glycoproteins and intestinal microvillus proteins such as MUC5AC, MUC6, MUC2, and villin (1,2). In the normal gastrointestinal tract, MUC5AC is present in the gastric foveolar epithelium, and MUC6 is detected in the mucous neck cells and pyloric glands. MUC2 is detected in the cytoplasm of goblet cells of the small intestine, colon, and intestinal metaplasia associated with chronic gastritis. Villin is present on the luminal surfaces of absorptive cells of the small intestine, colon, and intestinal metaplasia. In the normal pancreas, neither MUC5AC nor MUC2 is expressed (3,4), while MUC6 is found focally in the cytoplasm of normal acinar cells, and ductal epithelium (3,5,6). Villin immunoreactivity is located at the luminal surfaces of ductal and acinar cells (7,8). In several histological types of pancreatic tumors, MUC5AC and MUC2 have been frequently observed (3-5,9-11). MUC6 is sometimes detectable in mucinous cystic tumors, intraepithelial neoplasms and invasive ductal carcinomas (3,5), and villin has also been reported in the pancreatic tumors (7,8,12). We have previously examined the phenotype of gastric cancer cells using several phenotypic markers such as MUC5AC, MUC6, MUC2, and villin (13-15). Together with others, we have shown that combined evaluation of gastric and intestinal epithelial cell markers is clinically useful for predicting the outcome in patients with advanced gastric cancers (14,16). However, clinicopathologic significance of the expression of the same phenotypic markers in pancreatic tumors has yet to be clarified in detail. Several authors have demonstrated a correlation between prognosis and phenotypic markers in pancreatic tumors (4,17-21), but concrete conclusions have yet to be drawn.

The *Caudal*-related homeobox gene (Cdx) 2 is believed to be important for the maintenance of intestinal phenotypic expression (15,22-26). Several reports have pointed to a tumor-suppressor potential in human colorectal tumorigenesis (27-29). Using HT-29 colon carcinoma cells, Bai *et al* (30) have provided evidence that Cdx2 up-regulates transcription of p21/WAF1/CIP1, which plays a critical role in differentiation and tumor suppression. Cdx2 has been reported as a useful prognostic factor in gastric cancer cases as well (14,31). But despite two reports of its expression in pancreatic tumors,

Correspondence to: Dr Tetsuya Tsukamoto, Division of Oncological Pathology, Aichi Cancer Center Research Institute, 1-1 Kanokoden, Chikusa-ku, Nagoya 464-8681, Japan
E-mail: ttsukamt@aichi-cc.jp

*Contributed equally

Key words: pancreatic tumor, *Caudal*-related homeobox gene 2 (Cdx2), mucin phenotype

(12,32), it has remained unclear as to whether this has clinicopathologic significance.

In the present study, we therefore analyzed the expression of Cdx2 by immunohistochemistry in 77 pancreatic tumors, which were also evaluated histologically and phenotypically. Furthermore, interrelations with prognosis were examined in 30 pancreatic cancer cases.

Materials and methods

Samples and tissue collection. A total of 77 pancreatic tumors surgically resected at Aichi Cancer Center Hospital between 1988 and 2001 were examined. The patients consisted of 47 men and 30 women, aged 63.2±11.1 years (mean ± standard deviation). All specimens were fixed in 10% buffered formalin, processed routinely, and then sectioned and stained with hematoxylin and eosin (H&E) for histological examination. Classification was made according to the General Rules for the Study of Pancreatic Cancer (33). The tumors were classified into 19 mucinous cystic tumors (MCTs), 17 intraductal papillary-mucinous tumors (IPMTs), and 41 invasive ductal carcinomas (IDCs).

Immunohistochemistry. Immunohistochemical staining was carried out with monoclonal antibodies against the following antigens: MUC5AC (CLH2; 1:500, Novocastra Laboratories, Newcastle upon Tyne, UK); MUC6 (CLH5; 1:500, Novocastra Laboratories); MUC2 (Ccp58; 1:500, Novocastra Laboratories); and villin (clone 12; 1:20000, Transduction Laboratories, Lexington, KY). The precise procedures for immunohistochemical techniques were as previously described (14,15,26). Briefly, 4 mm-thick consecutive sections were deparaffinized and hydrated through a graded series of alcohols. After inhibition of endogenous peroxidase activity by immersion in 3% H_2O_2/methanol solution, antigen retrieval was carried out with 10 mM citrate buffer (pH 6.0) in a microwave oven for 10 min at 98°C. Then, sections were incubated with the primary antibodies. After thorough washing in phosphate-buffered saline (PBS), they were next incubated with biotinylated secondary antibody, and then with avidin-biotinylated horseradish peroxidase complex (Vectastain Elite ABC Kit, Vector Laboratories, Inc., Burlingame, CA). Finally, immune complexes were visualized by incubation with 0.05% 3,3'-diaminobenzidine tetrachloride (DAB) in the presence of 0.01% H_2O_2. Nuclear counterstaining was accomplished with Mayer's hematoxylin. We also examined expression of Cdx2 using an anti-Cdx2 monoclonal antibody (BioGenex, San Ramon, CA) with the same immunohistochemical approach as described previously (14,15,26,34). The results for each antibody staining were evaluated with reference to the percentage of positively stained cancer cells. A result was considered positive if ≥10% of the cells were stained.

Classification of phenotype. MUC5AC and MUC6 are markers of gastric epithelial cells, whereas MUC2 and villin are typical of the intestinal epithelial cell phenotype (13-16,26). Pancreatic tumors in which >10% of the section area consisted of either the gastric or the intestinal epithelial cell phenotype were classified as gastric (G type) or intestinal (I type) phenotype tumors, respectively. Those which showed both gastric and intestinal phenotypes were classified as gastric and intestinal mixed phenotype (GI type) tumors, while those showing neither gastric nor intestinal phenotypic expression were grouped as unclassified (N type).

Table I. Histological and phenotypic classification, and Cdx2 expression in pancreatic tumors.

Histological classification	Phenotypic classification[a]				
	G type	GI type	I type	N type	Total
MCTs	8 (7)	9 (8)	1 (1)	1 (1)	19 (17)
IPMTs	7 (1)	9 (7)	1 (1)	0 (0)	17 (9)
IDCs	24 (6)	11 (7)	1 (1)	5 (0)	41 (14)
Total	39 (14)	29 (22)	3 (3)	6 (1)	77 (40)

[a]The number of Cdx2-positive cases are given in parentheses. MCTs, mucinous cystic tumors; IPMTs, intraductal papillary-mucinous tumors; IDCs, invasive ductal carcinomas.

Statistical analysis. The data were analyzed by Fischer's exact test for differences between the groups. To determine the relative survival of patients, Cox's proportional-hazards regression model was used, and survival curves after surgery were drawn using the Kaplan-Meier method. The statistical comparison for survival was performed using the log-rank test. P-values <0.05 were considered statistically significant.

Results

Expression of gastric and intestinal phenotypic markers in MCTs, IPMTs, and IDCs. Expression of MUC5AC, MUC6, MUC2, and villin was demonstrated in 17 (89.5%), 10 (52.6%), 7 (36.8%), and 5 (26.3%) of 19 MCTs, respectively. Similarly, expression of MUC5AC, MUC6, MUC2, and villin was observed in 16 (94.1%), 12 (70.6%), 9 (52.9%), and 6 (35.3%) of 17 IPMTs. In 41 IDCs, the incidence of MUC5AC, MUC6, MUC2, and villin positivity was 35 (85.4%), 5 (12.2%), 8 (19.5%), and 8 (19.5%), respectively. Taking into account the combination of expression of these four markers, 77 pancreatic tumors were divided phenotypically into 39 G, 29 GI, 3 I, 6 N types, independent of the histological types (Table I). It was shown that 17 (89.5%) of 19 MCTs, 16 (94.1%) of 17 IPMTs, and 35 (85.4%) of 41 IDCs are judged to be positive for gastric phenotypic expression of either G or GI type. This was the case for 68 (88.3%) of the total 77 lesions.

Expression of Cdx2 in MCTs, IPMTs, and IDCs. Cdx2 nuclear staining was detected in intestinal phenotypic tumor cells, independent of the lesion histological type (Figs. 1 and 2). A strong association was observed between Cdx2 nuclear staining and intestinal phenotypic expression in the pancreatic tumors (p=0.0002, Table II). Most MCTs (89.5%) were judged to be Cdx2-positive, as well as 9 cases (52.9%) of 17 IPMTs. In the IDCs, totals of 14 and 27 cases were judged to be Cdx2-positive and Cdx2-negative, respectively (Table I).